J. Phys. C: Solid State Phys. **21** (1988) 2399–2411. Printed in the UK

The electronic structure of 1T-TaS_2 at room temperature and 120 K

R Manzke, O Anderson† and M Skibowski
Institut für Experimentalphysik, Universität Kiel, D-2300 Kiel, Federal Republic of Germany

Received 2 November 1987

Abstract. The experimental band structure of layered 1T-TaS_2 in the nearly commensurate phase at room temperature is investigated for the main symmetry directions, including three-dimensional effects, by angle-resolved photoemission with high energy and angle resolution and high absolute accuracy using He I and synchrotron radiation. In order to investigate the charge-density-wave (CDW) effects already present in the nearly commensurate phase, the room-temperature results are compared with measurements in the commensurate CDW state at 120 K. The dominant features in the electronic structure are described reasonably well by band structure calculations for the normal undistorted phase. Additional emission close to the Fermi energy can be assigned to CDW effects that strongly affect primarily the tantalum 5d band, which become very prominent at 120 K.

1. Introduction

Recent photoemission investigations on 1T-TaS_2 were mainly concerned with the unusual temperature behaviour, which is characterised by several structural phase transitions, and its commensurate charge-density-wave (CDW) state below about 200 K (Pollak *et al* 1981, Smith *et al* 1985). Theoretical work on these phenomena is in progress, but until now only simple model calculations have been applied to this problem (Smith *et al* 1985). On the other hand, for the normal undistorted phase of 1T-TaS_2 there exist several band structure calculations but only little experimental work; especially there is no complete experimental band structure with the resolution and accuracy attainable today, including possible three-dimensional effects.

Band structure calculations on 1T-TaS_2 by Mattheis (1973) have employed the augmented-plane-wave (APW) method and those by Myron and Freeman (1974) for the conduction bands only and Woolley and Wexler (1977) have employed the KKR method. All calculations agree well concerning the energies and dispersions of the bands. In the normal phase, where tantalum as the group Vb element is in the d^1 configuration, 1T-TaS_2 is found to be a metal. The calculated value of the indirect gap between the lowest d band at L and the lower-lying p bands at Γ is 1.3 eV.

The first angle-resolved photoemission spectroscopy (ARPES) measurements on 1T-TaS_2 for the ΓM direction were taken at 10.2 eV photon energy with relatively poor

† Present address: Schott Glaswerke, Hattenbergstrasse 10, D-6500 Mainz, Federal Republic of Germany.

0022-3719/88/122399 + 13 $02.50

resolution (Smith and Traum 1975), allowing only a rough comparison with the theoretical results. The authors did not observe any influence of CDW formation on the electronic structure. This work was extended for the ΓK direction by Mamy *et al* (1981) with 40 eV photon energy. Measurements taken with a display analyser (Pollak *et al* 1981), on the other hand, exhibit dramatic changes of the d band emission near E_F and the Ta 4f core level emission for the different CDW states. The d band emission near E_F in the commensurate CDW state at low temperature is investigated for the ΓM direction in a recent high-resolution ARPES work by Smith *et al* (1985).

In this investigation we present the complete electronic band structure of 1T-TaS_2 at room temperature for the main symmetry directions, including three-dimensional effects derived from angle-resolved photoemission with high resolution and absolute accuracy. We note that at room temperature 1T-TaS_2 has transformed into the nearly commensurate phase and the influence of the CDW on the electronic structure is already present in the vicinity of E_F. These effects will be worked out by applying the best energy and angle resolution. Measurements in the normal undistorted phase above 543 K are extremely difficult because this phase exists only in a narrow temperature range, and in this high-temperature region 1T-TaS_2 slowly transforms into the 2H modification (Bayliss *et al* 1983). So, our room-temperature results will be compared with theoretical ones for the normal phase. To consider the CDW effects we compare the room-temperature spectra with spectra at 120 K, where 1T-TaS_2 is in the commensurate CDW state.

2. Experimental aspects

1T-TaS_2 single crystals were grown from the elements by iodine-vapour transport in closed quartz tubes with a small excess of sulphur (3 mg cm^{-3}) by applying a temperature gradient of 860 to 760 °C. These preparation conditions are known to give the best stoichiometric samples. After a growth time of 40 days the tubes were quenched from about 750 °C in cold water, because 1T-TaS_2 is stable only at high temperature. The orientation and structure of the samples were controlled by standard x-ray techniques and by low-energy electron diffraction (LEED), the quality concerning the appearance of phase transitions by transport measurements. For the photoemission measurements, the crystals were mounted on an adjustable sample holder attached to a helium evaporation refrigerator and cleaved in ultra-high vacuum of about 10^{-8} Pa.

The photoemission spectra were taken with He I resonance radiation (21.2 eV) and synchrotron radiation (10–30 eV) from the DORIS II storage ring at HASYLAB in Hamburg. The electrons were detected by use of a 180° spherical analyser mounted on a goniometer, which is movable independently around two axes (improved Leybold Heraeus 3-DARES). These degrees of freedom allow a very accurate final sample adjustment, performed by taking spectra in small-angle steps around the critical points without moving the sample. The capability of this system has been demonstrated elsewhere (Anderson *et al* 1985, Manzke *et al* 1987). For the spectra shown here, an overall energy resolution of 70 and 35 meV and an angle resolution of ±0.5° were chosen.

3. Results and discussion

3.1. Electronic structure at room temperature

We first discuss the $k_\perp$ spectra in order to determine the ΓA band structure, the dispersion

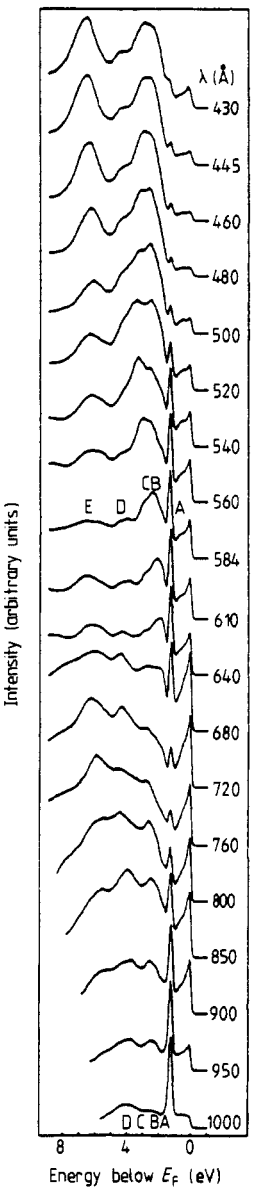

Figure 1. Energy distribution curves (EDC) taken at normal emission for ΓA direction at room temperature. Spectra are shown for 430 Å ≤ λ ≤ 1000 Å and scaled with respect to their absolute maxima. Peaks due to p valence band states are indicated by capital letters.

of which accounts for three-dimensional effects in these quasi-two-dimensional crystals owing to interactions not only parallel to the layers but also perpendicular. Energy distribution curves (EDC) of 1T-TaS_2, taken for different photon energies at normal emission ($k_{\parallel} = 0$) and 30° photon incidence angle with respect to the surface normal, are shown in figure 1. In all spectra one observes (i) relatively weak emission between 0 and 1 eV binding energy, which can be interpreted as being caused by the nearly commensurate CDW present in 1T-TaS_2 at room temperature because no occupied states are expected in the vicinity of E_F for the normal undistorted phase according to band

structure calculations (this will be discussed below in detail); and (ii) strong emission between 1 and 7 eV with at least six peaks due to the valence band p states. The maximum of the valence bands (3^- band in the notation of Mattheis (1973)) is formed in the spectra by the narrow peak A at 1.3 eV without any dispersion. At higher binding energies two structures (B and C) are observed between 2 and 3 eV with strong intensity variations. At 1000 Å these peaks lie very close together and are found separated for lower wavelength owing to the strong dispersion of peak C. Thus, peak C should be associated with the p_z-like 2^- band, for which the stronger dispersion with respect to $k_\perp$ is expected. For further identification of the 2^- band, we took an additional $k_\perp$ series of spectra with 60° photon incidence angle, for which the emission from the p_z-like 2^- band is weakly enhanced relative to the 30° series owing to matrix element effects. Peak B exhibits weak dispersion, a feature always present in the spectra of 1T structures at about 2 eV binding energy (Anderson *et al* 1988). Its origin can be explained either by lattice defects (vacancies on transition-metal sites) in these crystals (Pehlke and Schattke 1987), or by the 3^- band which will be discussed below. The dispersionless peak D and the more dispersive peak E should be due to the 3^+ and 1^+ bands, respectively. In some spectra it can be seen that these peaks are split into two subpeaks.

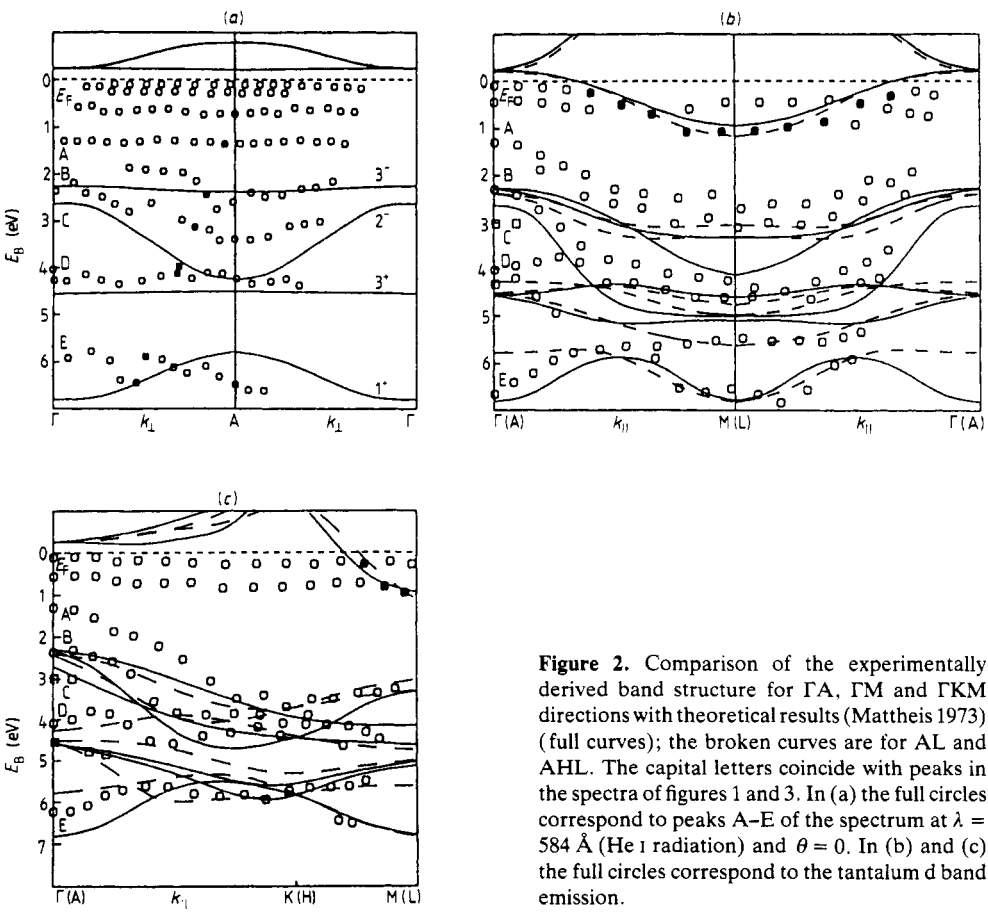

Figure 2. Comparison of the experimentally derived band structure for ΓA, ΓM and ΓKM directions with theoretical results (Mattheis 1973) (full curves); the broken curves are for AL and AHL. The capital letters coincide with peaks in the spectra of figures 1 and 3. In (a) the full circles correspond to peaks A–E of the spectrum at λ = 584 Å (He I radiation) and $\theta = 0$. In (b) and (c) the full circles correspond to the tantalum d band emission.

In order to determine quantitatively the initial-state dispersion relation $E_i(k)$ from the spectra of figure 1, we assume direct transitions into free-electron-like final-state bands in an inner potential V_0 with respect to the vacuum level. This can be viewed as a proper approximation for these layered crystals as suggested by LEED calculations (Pehlke and Schattke 1986a). Then the wavevector perpendicular to the surface is given within an extended zone scheme by

$$k_\perp = (1/\hbar)[2m(E_{\text{kin}} \cos^2 \theta + V_0)]^{1/2}.$$

For the parallel component of the wavevector we have

$$k_\parallel = (1/\hbar)(2mE_{\text{kin}} \sin^2 \theta)^{1/2}.$$

The inner potential is determined experimentally by fitting the extrema of the dispersive 2^- band (peak C) to critical points in the Brillouin zone (BZ). Maximum binding energy of 3.4 eV is found at about 560 Å, which is assumed to coincide with the BZ boundary at the A point. On the other hand, minimum binding energy of 2.2 eV is observed around 1000 Å, corresponding to the Γ point. From this we derive an inner potential $V_0 = 10$ eV for 1T-TaS_2. Note that this identification of the Γ and A points corresponds to the intensity variations in the dispersionless 3^- valence band (peak A) caused by the energy dependence of the transition matrix element, with intensity maxima around 1000 Å and 560 (figure 1) at high-symmetry points in the BZ (Γ, A).

With the knowledge of the high-symmetry points Γ and A, it is possible to compare quantitatively the experimentally derived band structure for the ΓA direction with theoretical results. This is shown in figure 2(*a*). One clearly finds a correspondence for the nearly dispersionless bands, 3^- and 3^+, with experimental bands at binding energies of 1.3 eV (A) and 4.2 eV (D), respectively. Besides this qualitative agreement, the deviations for the binding energies between experiment and calculation, 1 eV for the 3^- band and 0.3 eV for the 3^+ band, are large. As pointed out above, peak D is found experimentally as a double structure. This possibly indicates a lifting of the degeneracy of the 3^+ band. The binding energy of 2.2 eV at Γ of the dispersive 2^- band differs from the theoretical result by about 0.3 eV. Its experimental bandwidth of 1.2 eV is only slightly smaller than the calculated value of 1.6 eV. Thus, in comparison to 1T-$TiSe_2$ (Anderson *et al* 1985), the three-dimensional effects are more properly described in 1T-TaS_2 by Mattheis' (1973) calculations.

The 1^+ band at about 6 eV binding energy appearing as a broad double-peaked structure (peak E) in the spectra seems to be, at first sight, at variance with theory. But it apparently behaves similarly to the corresponding band found in other 1T-type crystals and can be interpreted to be an effect of the coupling of this initial state to two allowed final-state bands (Pehlke and Schattke 1986b).

Besides this qualitative good agreement between experiment and theory, significant additional emission is found in our spectra in the valence band region at about 2 eV (peak B) and between 0 and 1 eV binding energy. In a first explanation given above, peak B could be due to additional emission from defect states, in accordance with results for 1T-$TiSe_2$. On the other hand, the weak but distinct dispersion of peak B is in contrast to this explanation relying on almost non-interacting states. From figure 2(*a*) it can be seen that the binding energy of peak B coincides with the calculated 3^- band, thus suggesting that alternatively this peak is explainable by emission from the 3^- band by

spin–orbit splitting of about 1 eV not included in the calculation. As already mentioned, the structures between 0 and 1 eV binding energy in the normal emission spectra without any dispersion have no equivalent in the calculated electronic structure of the normal phase of 1T-TaS_2. For the calculated undistorted phase, all d bands should be located well above E_F. Since at room temperature 1T-TaS_2 has already transformed into the nearly commensurate phase, this substructure must be attributed to effects of the CDW.

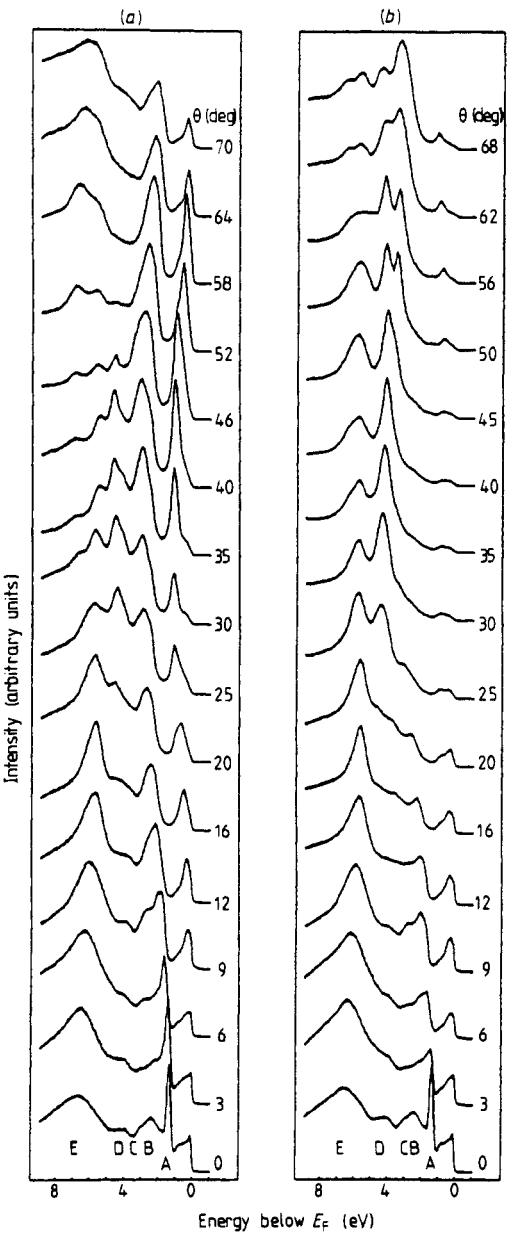

Figure 3. Spectral series of 1T-TaS_2 at room temperature for the high-symmetry directions ΓM (*a*) and ΓK (*b*). Peaks due to p valence band states are indicated by capital letters.

It becomes more distinct in the low-temperature spectra, which will be discussed in detail later (§ 3.3).

We now turn to the dispersion of the bands parallel to the layers, which has been partially investigated in previous work, but generally with less resolution and absolute accuracy. The EDC of 1T-TaS_2 at room temperature for different emission angles θ ($k_\parallel$ spectra) parallel to the high-symmetry directions ΓM and ΓK taken with He I radiation are shown in figure 3. At normal emission ($\theta = 0$) the peaks are indicated by the same capital letters used for the $k_\perp$ spectra. The valence band maximum of the sulphur 3p bands (peak A) is found as an intense and narrow emission at 1.3 eV binding energy for $\theta = 0$. With increasing θ parallel to ΓM it disperses to higher binding energy towards the BZ boundary at M ($\theta \simeq 30°$) and reversal in the second BZ. At higher binding energies the peaks B–E, due to the remaining S 3p bands, show distinct dispersions. Very clearly the double-peaked structure of peak D associated with the 3^+ band is observable and can be followed over the whole θ range where the two parts of this band exhibit quite different dispersions. Thus, the occurrence of the spin–orbit splitting of the 3^+ band, found experimentally also in the $k_\perp$ spectra, is strongly supported by the $k_\parallel$ series of figure 3. We also measured a series with θ parallel to the ΓM′ direction (not shown here). By comparing the ΓM and ΓM′ spectra, distinct variations in the intensities of the peaks are observable, whereas their energy positions are found to be unchanged. The ΓM′ series was used for further band structure analysis where the analysis of peaks in ΓM only became difficult. In the ΓK direction the p bands form a double-peaked structure at the BZ boundary K ($\theta \simeq 35°$) with binding energies of 4 and 6 eV. This double structure is found to be characteristic for all 1T-type transition-metal dichalcogenides (Anderson *et al* 1988, Anderson 1986).

In addition to the p band emission, all $k_\parallel$ spectra exhibit emission near E_F between 0 and 1 eV binding energy, similar to the $k_\perp$ series, which is very strong in the regime $9° < \theta < 58°$ in the ΓM series. This maximum intensity shows strong dispersion and reaches maximum binding energy at the M point (see figure 3(*a*)). This intense peak can be assigned to the Ta d band of the normal phase, which is obviously also strongly present in the nearly commensurate phase at room temperature. The behaviour of this band is considered to be responsible for the metallic character in the normal phase. On the other hand, the additional substructure (see also §§ 3.2 and 3.3) demonstrates the presence of the nearly commensurate CDW state. In the ΓM′ series (not shown here), the intensity of the d band emission is distinctly reduced. The decreased intensity of the d band emission for ΓM′ is due to matrix element effects (shadowing by the topmost chalcogen atoms (Smith and Traum 1975)).

In the ΓK spectra the emission between 0 and 1 eV is much weaker than in ΓM. This emission is absolutely in contrast to theoretical results of the normal phase for this direction, where the calculated d band is located well above E_F. Thus, we attribute this emission in accordance with our observations for ΓA and a previous investigation (Smith *et al* 1985) to effects caused by the CDW at room temperature. We note here that, also in undistorted 1T-type crystals, additional emission has been observed for the ΓK direction (de Boer *et al* 1984, Anderson *et al* 1988), the origin of which is not conclusively understood yet. But in these cases the emission is found to be weaker than in the case of TaS_2, discussed here, and seems to be very much pinned to E_F. Therefore it does not explain the substructure in the spectra shown in figure 3(*b*).

The comparison between the experimentally and theoretically derived band structure of 1T-TaS_2 for the ΓM and ΓK directions is given in figures 2(*b*) and (*c*). In addition to the theoretical bands for ΓM and ΓKM, we inserted the bands for AL and AHL (Mattheis

1973) to account for $k_\perp$ in the spectra taken with He I radiation. In the $k_\perp$ band structure of figure 2(*a*) the bands corresponding to peaks in the spectrum taken with 584 Å radiation are indicated by black dots. These correspond to bands at $\Gamma(\theta = 0)$ in figure 2(*b*) and (*c*). Thus, for band A the $k_\parallel$ dispersion starts near the A point whereas for band E it starts nearly in the middle between Γ and A. In detail, the dispersion of peak A is in good agreement with that of the calculated $A_3^- L_1^-$ band. However, its energy location differs from the calculated values by about 1 eV. It is remarkable that the dispersion of peak B follows that of the $A_3^- L_2^-$ band for larger $k_\parallel$ values. Near A, the calculated $A_3^- L_1^-$ and $A_3^- L_2^-$ bands degenerate, whereas the experiment finds peak B separated from peak A by about 1 eV. Thus, the spin–orbit splitting of the 3^- band near Γ (or A), discussed above, seems to be evident from the experimental data. Regarding the remaining p bands, it can be pointed out that peak E follows the dispersion of the $\Gamma_1^+ M_1^+$ band, because with respect to ΓA peak E is nearer the Γ point, and peak D

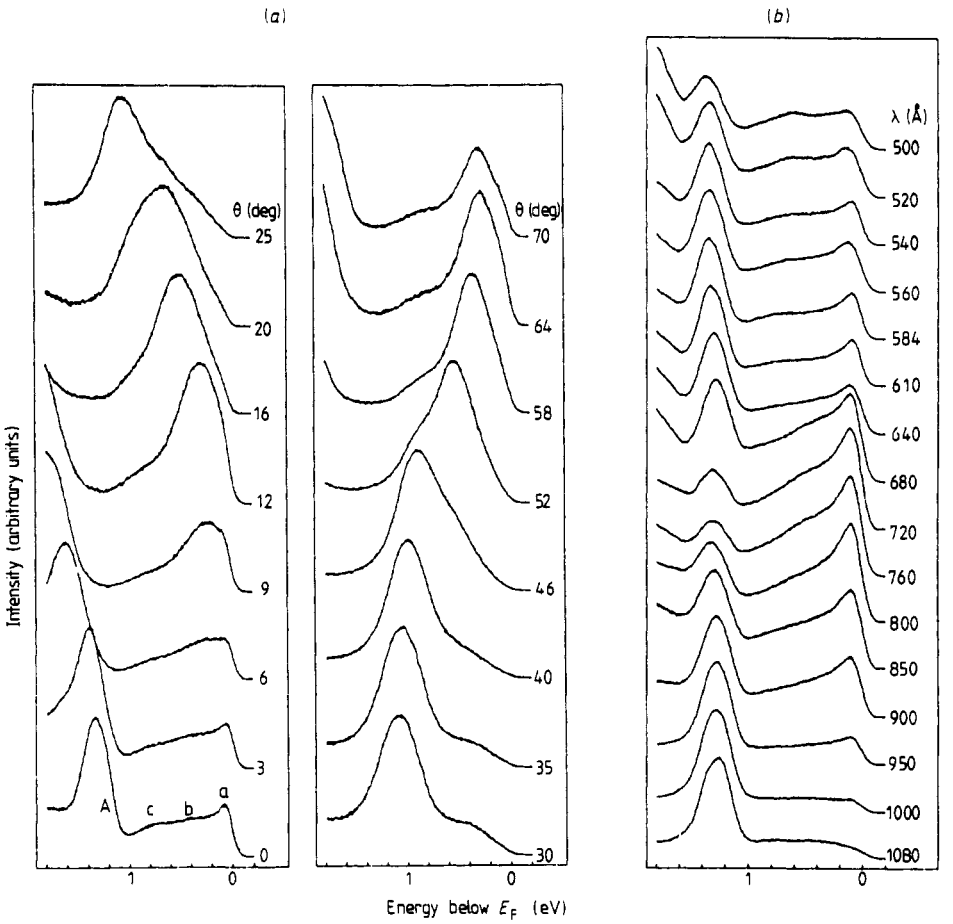

Figure 4. High-resolution spectra at room temperature for ΓM direction taken with He I radiation (*a*) and ΓA direction with synchrotron radiation (*b*). The photon-energy-dependent spectra (*b*) were taken at normal emission ($\theta = 0$). Peak A indicates the p valence band maximum; peaks a–c are the CDW-induced structures (see text).

follows the dispersion of the $\Gamma_3^+ M_2^-$ or $A_3^+ L_2^-$ bands, which are nearly identical because of their negligible $k_\perp$ dispersion. The second structure of peak D follows the dispersion of the $\Gamma_3^+ M_2^+$ (or $A_3^+ L_2^+$) band and cuts the dispersive peak C ($A_2^- L_1^+$ band) near the middle of the BZ. Regarding peak C, with respect to $k_\perp$ it is located nearer to the A point but the amount of dispersion observed experimentally coincides better with that of the theoretical $\Gamma_2^- M_1^+$ band.

In the vicinity of E_F the tantalum 5d band and the CDW-induced structures show up. The dispersion of the strong d band is clearly observable in ΓM (AL) and MK (HL) directions (black dots in figures 2(*b*) and (*c*)) and it follows excellently the behaviour expected from theory for the normal phase. It cuts E_F near the middle of the BZ and reaches maximum binding energy of 1.1 eV at M (L). Thus, the measured occupied d electron bandwidth of 1.1 eV compares very well with the calculated one (e.g. 1.16 eV by Woolley and Wexler (1977)). Previous photoemission studies determined this bandwidth to be 1.5 eV (Traum *et al* 1974) and about 1.1 eV (Pollak *et al* 1981).

Our experimental value of the indirect p/d gap between Γ and L is 0.2 eV (see also the high-resolution results of figure 5). It is clear from the discussion above for the 3^- band that this experimental value is very different from the calculated p/d gaps of 1.0 and 1.3 eV by Woolley and Wexler (1977) and Mattheis (1973), respectively. Efforts to use a better self-consistent potential for the calculations, which would reduce the p/d gap (Woolley and Wexler 1977), have not been published yet.

3.2. High-resolution experiments at room temperature

In order to account for the CDW effects in the nearly commensurate state at room temperature on the tantalum 5d band structure of the undistorted phase, we applied our best attainable energy resolution of 35 meV to investigate the emissions in the vicinity of E_F. In figure 4 a series of photon-energy-dependent normal emission spectra ($k_\perp \hat{=}$

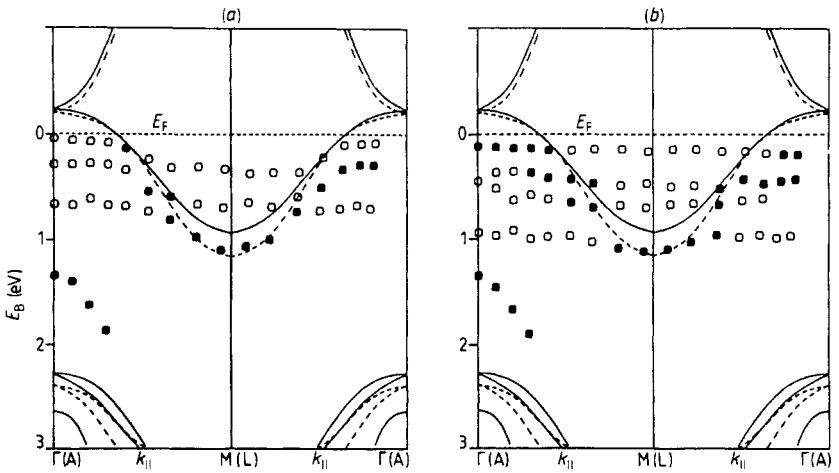

Figure 5. Comparison between the experimental band structure derived from the high-resolution spectra for ΓM direction at room temperature (*a*) and at 120 K (*b*). For details see text.

ΓA) and spectra for k parallel to the ΓM direction with He I radiation are shown. Regarding first the $k_\parallel$ spectra of figure 4(*a*), it can be clearly seen that the strongly dispersing intense peak cuts E_F at about $\theta = 9°$. It disperses to higher binding energies down to 1.1 eV at the zone boundary M (L) ($\theta \simeq 30°$) and reversal in the second BZ. At 1.3 eV binding energy one finds peak A due to the valence band maximum of p states for $\theta = 0°$. Besides the intense d band emission, three additional structures with weak intensity can be resolved in the spectra.

In figure 5(*a*) the experimental band structure, derived from the high-resolution spectra of figure 4(*a*), is shown together with the calculated results of Mattheis (1973). The strong d band emission and the maximum of the p valence band are indicated by full circles. Considering the dispersive tantalum d band, the agreement between experiment and the calculated $A_3^+ L_1^+$ band is excellent. In addition the p/d gap is shown, which differs strongly from theory, as already discussed above. The additional weak structures are indicated by open circles. They do not show any dispersion and should be attributed to CDW effects.

The simultaneous occurrence of d band behaviour of the undistorted normal phase, visualising the centre of gravity for the entire d emission, and the CDW phase effects, manifesting themselves as weak side bands in the room-temperature spectra, directly supports a domain model proposed to understand the nearly commensurate CDW state ($1T_2$ phase) of 1T-TaS_2 (McMillan 1976, Chapman and Colella 1985, van Landuyt 1980). In this model the microstructure of this phase consists of domains with perfectly locked-in CDW separated by domain walls (discommensurations), across which the CDW phase changes rapidly. Obviously, at room temperature this phase reflects more the electronic structure of the undistorted normal phase. With decreasing temperature the commensurate domains are viewed to grow in size relative to the discommensurations, until the whole crystal transforms into the commensurate $1T_3$ phase below $T_c \simeq 190$ K. Concerning the electronic structure, the influence of the CDW causes changes in the d band region close to E_F and explains the additional dispersionless structures in our spectra between 0 and 1 eV binding energy.

In the normal-emission ($k_\perp$) spectra of figure 4(*b*) all structures between 0 and 1 eV have to be attributed to CDW effects because there exists no equivalent in the band structure of the normal 1T phase. By fitting this energy regime using Gaussian profiles, we had to take at least three (a, b, c) dispersionless structures, similar to the ΓM direction. In addition, this series nicely shows the minimum of intensity of the p valence band maximum at about 760 Å interpreted above as being related to matrix element effects. For radiation of 760 Å and the binding energy of peak A of 1.3 eV, the excitation, with respect to $k_\perp$, is found to occur nearly in the middle between the high-symmetry points Γ and A where the combined density of states, in comparison to Γ and A, is expected to be small (see also figure 2(*a*)).

3.3. High-resolution experiments at 120 K

In this section additional support for the CDW model will be given by studying the features at 120 K in the commensurate $1T_3$ phase far below the transition temperature, $T_c \simeq$ 190 K. In figure 6 the high-resolution spectra near E_F at 120 K are shown. Besides the p valence band maximum (peak A) the CDW-induced structures are found to be strongly enhanced, now exhibiting additional distinct fine structure. Regarding first the low-temperature spectra parallel to ΓM, the p valence band maximum disperses with increasing θ to higher binding energies and reversal in the second, unreconstructed BZ, which

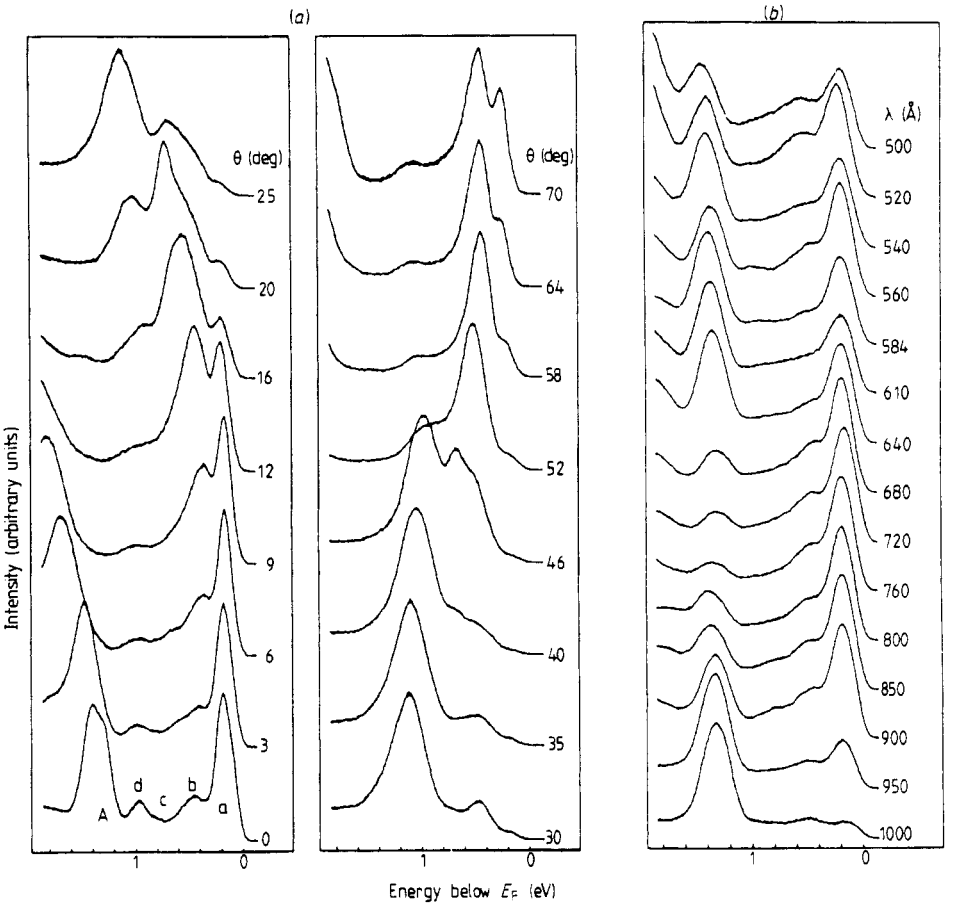

Figure 6. High-resolution spectra at 120 K for ΓM direction taken with He I radiation (*a*) and ΓA direction with synchrotron radiation (*b*). Here E_F denotes the experimental Fermi level.

is indicated by the peak at about 1.8 eV of the $\theta = 70°$ spectrum, which is near the Γ point of the second BZ. The periodicity of the dispersion of peak A due to the unreconstructed crystal is in line with our observation that the electronic properties of the p valence bands are obviously not much affected by the CDW formation.

The three structures a–c due to the commensurate CDW now form distinct maxima and an additional peak d clearly shows up. In comparison with the room-temperature spectra, especially the intensity of peak a is strongly enhanced, exhibiting strong intensity variations with θ, and is found to be shifted below E_F by about 200 meV due to the opening of an energy gap, so that below T_c 1T-TaS_2 becomes semiconducting. This is in agreement with the previous analysis of Smith *et al* (1985). With increasing emission angle θ the CDW-induced peaks show no dispersion but all exhibit remarkable intensity variations. The variation of the maximum intensity with θ, surprisingly, follows the dispersion of the d band of the unreconstructed phase. This is shown in figure 5(*b*) where the dispersionless CDW-induced peaks are indicated by open circles and the maximum of intensity in the regime 0 to 1 eV is given by full circles.

The behaviour of the CDW-induced bands near E_F for the ΓA direction is shown in figure 6(*b*). The energy gap is observed in all normal emission spectra. This confirms the semiconducting behaviour of 1T–TaS_2 in the $1T_3$ phase. The intensities of the structures between 0 and 1 eV are enhanced, especially that of peak a (see also figure 4(*b*)), and their dispersions are negligible, emphasising their two-dimensional character. A comparison of peak a with the band structure of the normal phase demonstrates that the dispersionless 3^+ band, found in the normal phase above E_F, has been shifted below E_F in the commensurate phase. This behaviour is already indicated in the spectra of the $1T_2$ phase of figure 4(*b*).

4. Conclusions

We have investigated in detail the experimental band structure of 1T-TaS_2 at room temperature. This can be compared with theoretical results taking into account also the charge-density-wave-induced effects in the spectra of the nearly commensurate ($1T_2$) phase. Qualitatively, the calculations are in reasonable agreement with the experiments, but the observed additional bands and large quantitative deviations call for new theoretical investigations.

Regarding the CDW-induced structures between 0 and 1 eV in the spectra of the nearly commensurate phase and the fact that the p valence bands and the averaged d band emission impressively behave as in the normal phase, our data yield strong evidence for the proposed presence of domains with locked-in CDW.

In addition to the nearly commensurate phase, the CDW-induced structures are found to be strongly enhanced in the commensurate CDW state at 120 K. A band gap referred to E_F of about 200 meV is derived for the ΓM as well as for the ΓA direction, demonstrating that the whole crystal has transformed to a semiconductor, in agreement with conductivity experiments. It remains a puzzle why even in the low-temperature $1T_3$ phase the electronic structure characteristic of the normal phase, especially the intensity modulation associated with the d band dispersion between 0 and 1 eV, is still present in the spectra.

Acknowledgments

We thank W Krüger for sample preparation and B Pfalzgraf for the transport measurements. This work was supported by the Bundesministerium für Forschung und Technologie under Project No 05 301 AAI.

References

Anderson O 1986 *PhD Thesis* University of Kiel
Anderson O, Manzke R and Skibowski M 1985 *Phys. Rev. Lett.* **55** 2188
—— 1988 to be published
Bayliss S C, Clarke A and Liang W Y 1983 *J. Phys. C: Solid State Phys.* **16** L831
Chapman L D and Colella R 1985 *Phys. Rev.* B **32** 2233
de Boer D K G, van Bruggen C F, Bus G W, Coehoorn R, Haas C, Sawatzky G A, Myron H W, Norman D and Padmore H 1984 *Phys. Rev.* B **29** 6797

McMillan W L 1976 *Phys. Rev.* B **14** 1496
Mamy R, Thiry P, Vachier G and Couget A 1981 *J. Physique Lett.* **42** L79
Manzke R, Barnscheidt H P, Janowitz C and Skibowski M 1987 *Phys. Rev. Lett.* **58** 610
Mattheis L E 1973 *Phys. Rev.* B **8** 3719
Myron H W and Freeman A J 1974 *Phys. Rev.* B **9** 481
Pehlke E and Schattke W 1986a *Surf. Sci.* **173** 20
—— 1986b *Verh. Dtsch. Phys. Ges. (VI)* **21** 1356
—— 1987 *Z. Phys.* B **66** 31
Pollak R A, Eastman D E, Himpsel F J, Heimann P and Reihl B 1981 *Phys. Rev.* B **24** 7435
Smith N V, Kevan S D and DiSalvo F J 1985 *J. Phys. C: Solid State Phys.* **18** 3175
Smith N V and Traum M M 1975 *Phys. Rev.* B **11** 2087
Traum M M, Smith N V and DiSalvo F J 1974 *Phys. Rev. Lett.* **32** 1241
van Landuyt J 1980 *Physica* B **99** 12
Woolley A M and Wexler G 1977 *J. Phys. C: Solid State Phys.* **10** 2601